UCIRVINE

Preliminary findings from 2023 indicate mesquite groundwater use near the Borrego Sink

Project Update

29 February 2024

Product of the *Groundwater Dependent Ecosystems (GDE) Identification, Assessment, and Monitoring Program* (hereafter 'the GDE Project')



Prepared by:

Laurel Brigham, UC Irvine

Nikki Fiore, UC Irvine

Research Team:

Laurel Brigham, UC Irvine

Nikki Fiore, UC Irvine

David Garmon, Tubb Canyon Desert Conservancy

Robert Staehle, Tubb Canyon Desert Conservancy

Lori Paul, Tubb Canyon Desert Conservancy

Daniel Donovan, SD Natural History Museum

Jon Rebman, SD Natural History Museum

Travis Huxman, UC Irvine

UCIrvine

To: Geoff Poole, General Manager, Borrego Water District; and
Chris Martinez, Engineering Geologist, California Department of Water Resources, Proposition 68 Sustainable Groundwater Management Grant Program

From: Travis Huxman, Chair, Department of Ecology and Evolutionary Biology, University of California, Irvine

Subject: Proposition 68 Project Update summarizing preliminary findings regarding groundwater dependent ecosystems in the Borrego Springs Subbasin.

We are pleased to share the attached project update "Preliminary findings from 2023 indicate mesquite groundwater use near the Borrego Sink." This is in satisfaction of Task 4a in our proposal and Work Plan. We will be sharing this document with the Borrego Springs Watermaster for consideration by their appropriate subcommittees and stakeholders in the basin.

This document has undergone multiple iterations of scientific and editorial review, and we are confident in the methods we employed in our analysis and the conclusions drawn regarding groundwater dependent ecosystems in the basin. However, this project update is focused on preliminary result dissemination and we anticipate further insights to come to light, from our project, from you, and from other stakeholders within the basin. These insights will shape the planning and progress of our ongoing work on the project and the activities of stakeholders in the basin, including potentially the Watermaster, who is focused on a contemporary estimation of sustainable yield in the current year.

We look forward to your comments, questions, and assistance disseminating this document through your website.

UCIRVINE

Executive Summary

- Our updated mapping using supervised image classification identified 350.1 acres of live mesquite tree canopy in the Borrego Springs Subbasin at the implementation of the Sustainable Groundwater Management Act in 2015.
- 1,800 acres of mesquite bosque habitat, a potential Groundwater Dependent Ecosystem (GDE), was mapped with this new analysis near the Borrego Sink.
- Results from our first year of measurements and remote sensing analyses are consistent with groundwater use across much of the mesquite bosque habitat near the Borrego Sink.
- 187 native plant species were detected in the mesquite bosque habitat in the vicinity of Borrego Sink, 12 of the native plant species are threatened or endangered; a growing number of animal species are being documented.
- An initial estimate of groundwater use by this habitat is 515 - 557 acre-feet (af) annually.
- Growing season project priorities include wildlife camera internships, expanded spatial sampling of isotopes, and deployment of micrometeorological sensors to directly measure evapotranspiration.

Introduction

In our March 2023 technical memorandum released in March 2023 by the Prop. 68 Groundwater Dependent Ecosystem Identification, Assessment, and Monitoring Program, we highlighted the need for a higher quality map of the mesquite bosque near the Borrego Sink and remote sensing analyses to support decision-making surrounding the implementation of the Groundwater Management Plan for the critically overdrafted Borrego Springs Subbasin (UCI, 2023 Technical Memorandum). Our memorandum outlined plans for field-collected isotopic analyses and other plant-and-ecosystem assessments to evaluate whether the mesquite bosque near the Borrego Sink is a groundwater dependent ecosystem (GDE). Here we present the most recent year's efforts to address these goals. This included extensive ecological field work and comprehensive remote sensing analyses on the mesquite bosque near the Borrego Sink and at a comparison site, near Clark Dry Lake. The comparison site is located in an adjacent basin (Ocotillo-Clark Valley Basin) which has not experienced significant declines in groundwater levels (groundwater is within 25 feet of the surface) and allows us to identify how mesquite with such access perform. In this document, we summarize these analyses to provide insights regarding the presence of a GDE in the Borrego Springs Subbasin, preliminary estimates of its spatial extent, and a first-pass estimate of its impacts on the basin water budget. Expanded descriptions of activities and analyses will continue to be communicated in our next project update to be published on the Steele/Burnand Anza-Borrego Desert Research Center website (*anticipated summer 2024*).

1. Mapping of mesquite bosque habitat constrained by live tree distribution yields 1,800 acres of live mesquite

To develop more accurate mapping of potential GDE we first conducted image classification of aerial images from 2016 to identify live mesquite trees (*Neltuma odorata* [formerly *Prosopis glandulosa*]) in the Borrego Springs Subbasin near the Borrego Sink (see Appendix A for theory and methods). We then used the classification procut to produce a baseline map of mesquite bosque habitat. This map includes the plant community, inclusive of interstitial spaces and associated species, which we now refer to as our 2016 Sustainable Groundwater Management Act (SGMA) Implementation Map.

The classification of aerial images from 2016 detected 350.1 acres of live mesquite tree canopy near the Borrego Sink (Fig. 1) which resulted in 1,800 acres of mesquite bosque habitat (Fig. 2). At our Clark Dry Lake comparison, image classification detected 86.2 acres (Fig. 3) of live mesquite tree canopy and 220 acres of mesquite bosque habitat.

There have been a number of different reports of mesquite bosque spatial extent in the region over the last several decades from different environmental reports relevant to groundwater management. Our 2023 Technical Memorandum highlighted the need for a contemporary map reflecting mesquite bosque distribution, given the most recent map comes from the County of San Diego in 1995 (SanGIS 2022). Compared to that 1995 effort, our 2016 SGMA Implementation Map indicates a reduction in mesquite area in the Borrego Springs Subbasin near the Borrego Sink. While the reduction in mesquite bosque area is likely attributed in part to mesquite mortality, it is important to consider differences in data quality, methodology, and the timing of data acquisition when comparing the 1995 map to our 2016 SGMA Implementation Map. In 1995, available satellite imagery was of a lower resolution and this habitat map was created by hand-drawing outlines where vegetation appeared to change, which resulted in a coarse assessment. The value in our mapping approach is that it provides for a more quantitatively reliable estimate of change detection moving forward in time relative to the implementation of SGMA in 2015, utilizing reliable, high-quality images.

Flora and fauna assessments near Borrego Sink and Clark Dry Lake indicate the mesquite bosques support a great deal of life. We detected 208 plant species in the Borrego Springs Subbasin in the vicinity of Borrego Sink, through both on-the-ground surveys and herbarium searches. Of these, there were 187 native plant species, 12 of which are threatened or endangered. Preliminary bird surveys were conducted in December and will be conducted again in mid-February. Wildlife camera data from June 2023 to present is being processed. Our next project update will expand on this summary.

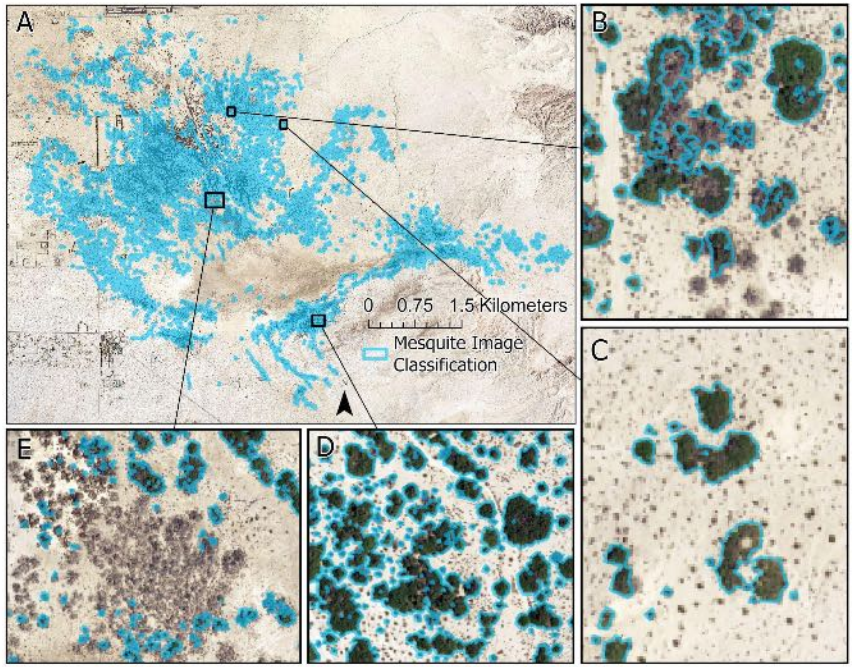


Figure 1. Image classification of mesquite in the Borrego Springs Subbasin near the Borrego Sink. The analysis discriminates between live and dead mesquite to effectively estimate individual, functional plants. Live mesquite identified through image classification are outlined in turquoise. Insets B and E highlight how dead mesquite (the brown areas in the map) are not included by the image classification. Insets D and C demonstrate the high performance of the classification in designating individual trees in dense and sparse settings, respectively. Base imagery from the National Agriculture Imagery Program (NAIP) taken 22 - 23 April 2016.

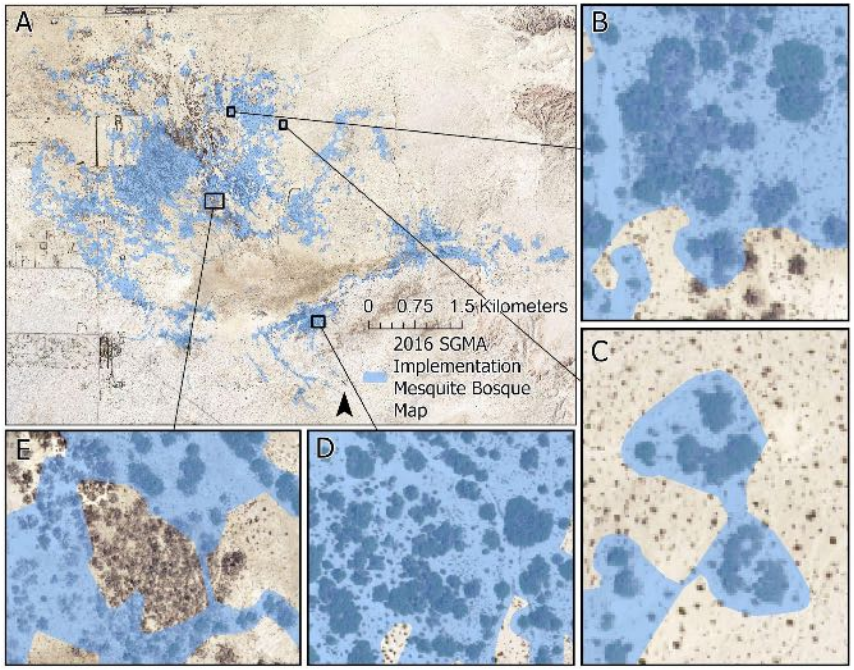


Figure 2. Mesquite bosque mapping in the Borrego Springs Subbasin near the Borrego Sink using image classification on 2016 aerial imagery illustrated in Fig. 1. Blue shaded portions of the map identify inclusive habitat (live canopy-covered ground area, inter-canopy ground area, and associated other plant species). The insets represent the same areas as Figure 1 and demonstrate how habitat is delineated in clustered (B), sparse (C), dense (D), and live-dead mosaic (E), examples of mesquite distribution. Base imagery from the National Agriculture Imagery Program (NAIP) taken 22 - 23 April 2016.

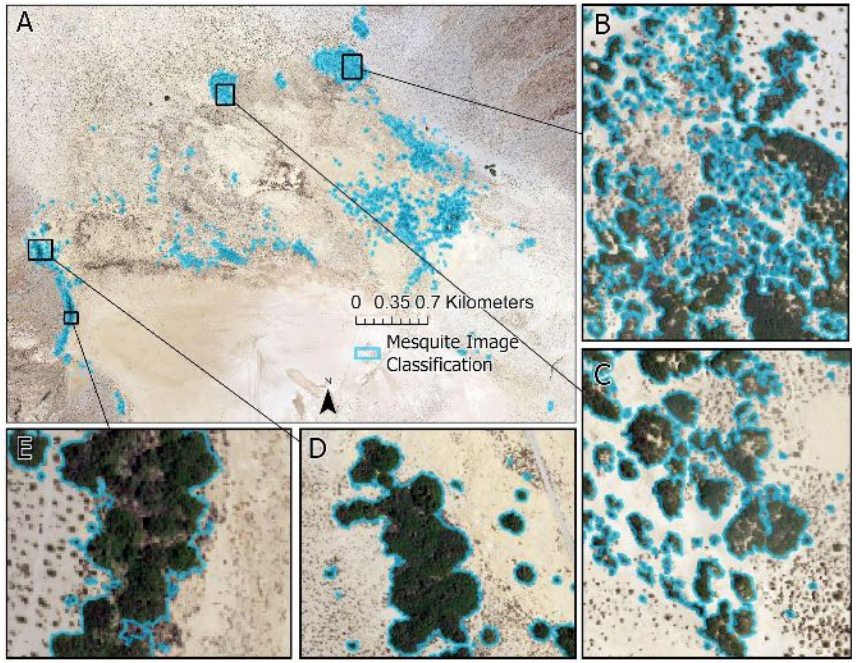


Figure 3. Image classification of mesquite at the Clark Dry Lake comparison site. The analysis discriminates between live and dead mesquite to more effectively estimate individual, functional plants. Insets highlight the high performance of the classification in designating individual trees in dense (B and C) and clustered (E and D) arrangements. Live mesquite identified through image classification are outlined in turquoise. Base imagery from the National Agriculture Imagery Program (NAIP) taken 22 - 23 April 2016.

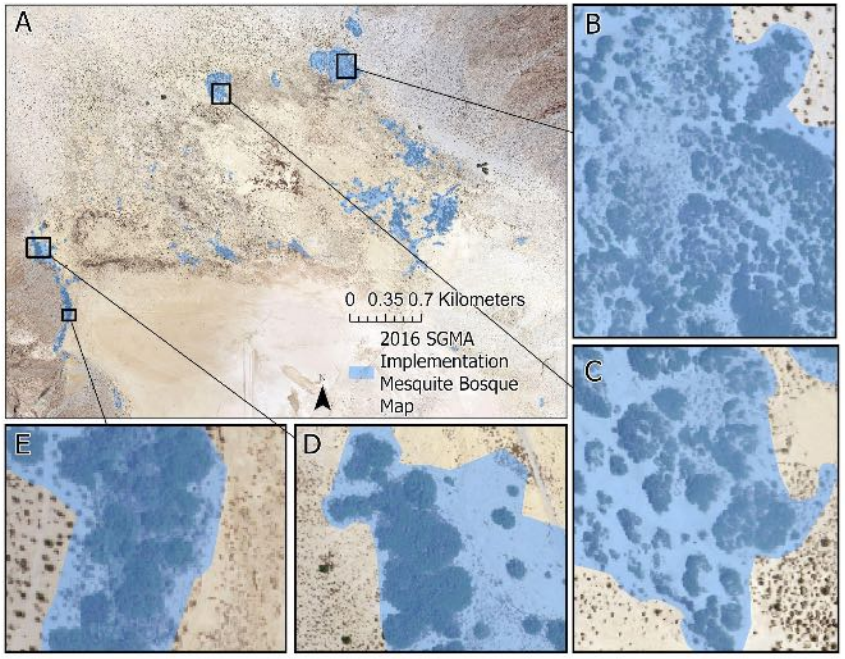


Figure 4. Mesquite bosque mapping for the Clark Dry Lake comparison site using image classification on 2016 aerial imagery. Blue shaded portions of the map identify inclusive habitat (live canopy-covered ground area, inter-canopy ground area, and associated other plant species). The insets cover the same area as Figure 3 and demonstrate how habitat is delineated in dense (B and C) and clustered (E and D) mesquite distribution. Base imagery from the National Agriculture Imagery Program (NAIP) taken 22 - 23 April 2016.

2. Remote sensing data indicates groundwater use by mesquite near the Borrego Sink

Initial studies during the Groundwater Management Planning process in Borrego Springs Subbasin were relatively simplistic due to time, data, and resource limitations. New information collected from more modern instrumentation platforms, including aerial-derived photographs and satellite-based spectroscopy, along with consensus frameworks for assessment in the scientific literature (see below), offer a means to better investigate the habitats identified through our mapping for behavior consistent with groundwater use. We employed three temporal and spatial approaches to systematically evaluate the behavior of the vegetation in response to ecosystem water availability at the Borrego Springs mesquite bosque near the Borrego Sink (the potential GDE), the Clark Dry Lake mesquite bosque (a known GDE), and a selected nearby non-GDE habitat (see Appendix B for theory and methods). Within each analysis, mesquite bosque habitat in Borrego Springs met assumptions of GDE behavior consistent with the habitat relying on access to groundwater (Table 1).

The three approaches rely on the "green island" conceptual framework used in the detection of GDEs through remote sensing (Eamus et al. 2015). This method compares vegetation characteristics between areas with unknown access to groundwater and those with and without access. These comparisons can occur at a single time point, across seasons, or over annual cycles. For instance, during extended dry periods (once near-surface soil water has been depleted), vegetation accessing groundwater tends to maintain better health and greenness than vegetation relying solely on the little remaining water held in high tension within the soil column. Vegetation with access to groundwater is less affected by dry surface soil conditions. Consequently, vegetation that remains physiologically active despite extended dry conditions is likely a GDE. In Approach 1 (Table 1), we found that 22% of mesquite bosque habitat pixels in Borrego Springs exhibited steady or increasing mesquite greenness or growth (as indicated by tau ≥ 0) during an extended dry period, which could only be supported by reliable access to groundwater (see Appendix B). Leaf-level measurements of plant water status assessed through predawn water potential support this interpretation based on the similarity between mesquite at the Borrego Sink (mean ± SD; -1.85 ± 0.34 MPa) and at Clark Dry Lake (-1.59 ± 0.43 MPa). In Figure 5, we present a map of GDE likelihood based on Approach 1 results, pinpointing hotspots of GDE behavior across the habitat. Approaches 2 and 3 were also consistent with the logic behind their specific expectation of GDE behavior and projections of areal extent of the GDE (see Appendix B).

Table 2. Summary of remote sensing approaches used to assess groundwater dependency for the potential GDE (Borrego Springs), the known GDE (Clark Dry Lake), and the non-GDE. Each approach uses remotely sensed Normalized Difference Vegetation Index (NDVI) as a proxy for plant health and productivity (see Appendix B for details). Approach 1 uses Mann Kendall's tau to determine if NDVI increases or remains stable across a dry period, indicating groundwater access. Approach 2 uses maximum NDVI to quantify how much live vegetation persists during dry periods, indicating groundwater access. Approach 3 uses cumulative NDVI (the sum of NDVI throughout the water year) to assess annual productivity, with values greater than the non-GDE indicating groundwater access. Each approach uses a different time period in 2023 to highlight behavior consistent with groundwater dependency throughout the year.

		Borrego Springs		Clark Dry Lake		Non-GDE	
Approach	**Assumption**	**Overall Summary**	**Indication of a GDE**	**Overall Summary**	**Indication of a GDE**	**Overall Summary**	**Indication of a GDE**
#1. Change in NDVI across an extended dry period	GDE should maintain or increase NDVI across the dry period due to access to groundwater (tau ≥ 0)	Assumption met	Yes	Assumption met	Yes	Assumption NOT met	No
#2. Comparison of maximum NDVI across dry period	GDE should have higher NDVI across dry periods than non-GDE due to access to groundwater	Assumption met	Yes	Assumption met	Yes	Assumption NOT met	No
#3. Comparison of cumulative NDVI across 2023	GDE should have higher cumulative NDVI than non-GDE due to the potential to accumulate biomass throughout the year due to access to groundwater	Assumption met	Yes	Assumption met	Yes	Assumption NOT met	No

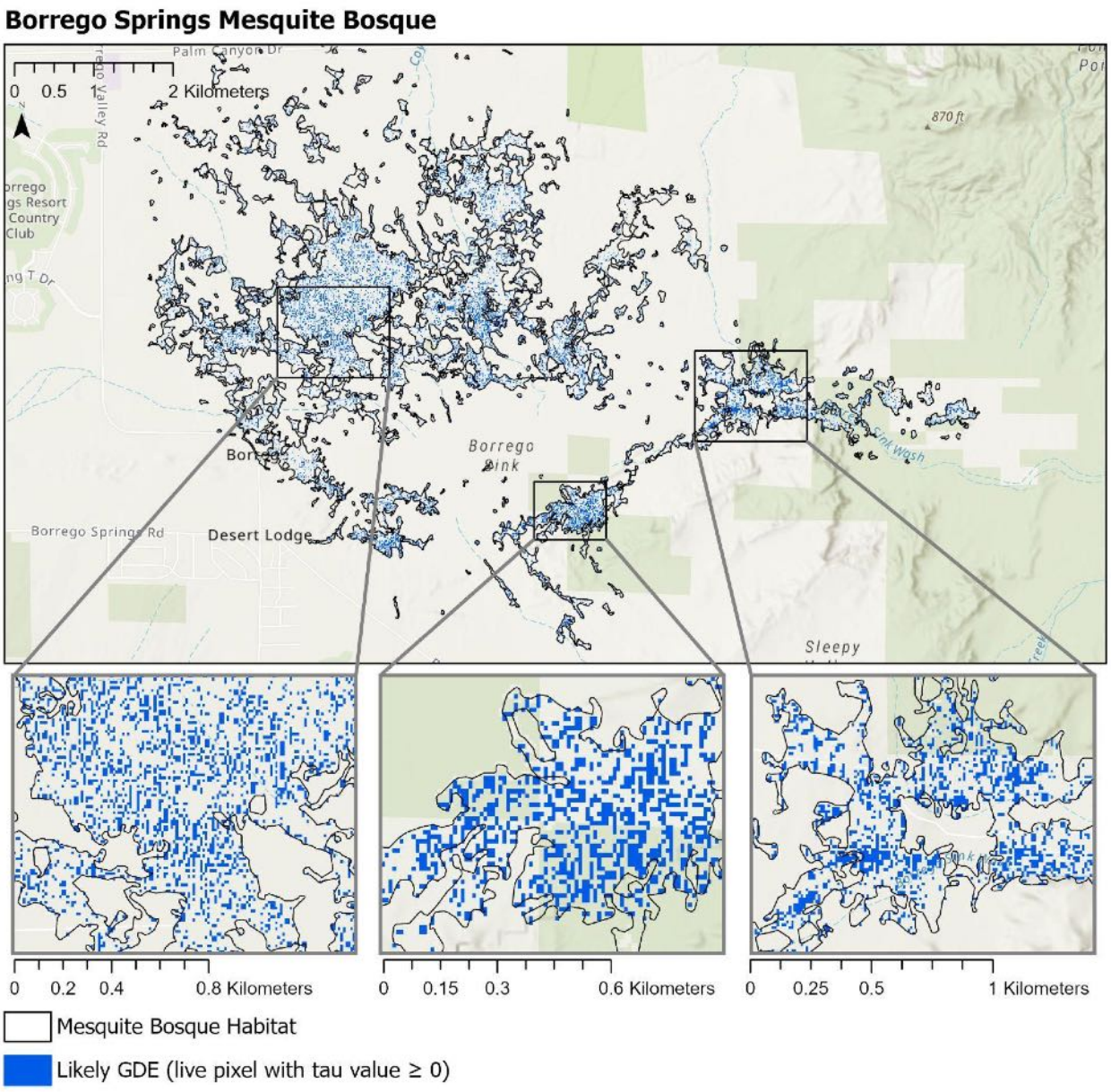


Figure 5. Map of the spatial extent of GDE behavior identified in Approach 1, which analyzes the change in NDVI across an extended dry period (May 21, 2023- June 20, 2023) for the Borrego Springs mesquite bosque using Mann Kendall's tau. Positive tau indicates an increase in NDVI and tau=0 indicates that NDVI remained stable across the dry period, both of which could only be supported by groundwater access. Areas shown in blue indicate live vegetation that had tau values ≥ 0, illustrating hotspots of GDE behavior throughout most of the Borrego Springs mesquite bosque habitat (see Appendix B for full methods).

3. Evapotranspiration estimates are consistent with groundwater use by mesquite near the Borrego Sink

The studies informing groundwater management planning in the Borrego Springs Subbasin previously dismissed potential presence of GDEs. Consequently, decision-makers generally assumed that evapotranspiration from non-irrigated landscapes equated to localized annual precipitation and did not significantly impact changes in groundwater storage. Given that our new mapping products and remote sensing analyses find land surface areas with GDE-consistent behavior, we have begun investigating potential groundwater-use by mesquite. To estimate groundwater transpiration by mesquite, we used the water balance equation proposed by Eamus et al. (2016), which states that:

$$\text{Groundwater transpiration } (ET_{gw}) = \text{Evapotranspiration (ET)} - \text{Precipitation} \quad (1)$$

We calculated groundwater transpiration (ET_{gw}) by subtraction of estimates of ET and precipitation using OpenET, which provides open-access satellite-based precipitation and ET data (Melton et al. 2022; Appendix Table C1, Transpiration of Vegetation of Interest). Live mesquite ET_{gw} near the Borrego Sink (mean ± SD; 1.53 ± 0.06 af per acre) and at Clark Dry Lake (1.69 ± 0.13 af per acre) were similar, and provide additional evidence of groundwater use near the Sink. These estimates of groundwater transpiration per acre can be scaled up using the acreage of live mesquite identified during image classification. Groundwater transpiration was estimated at 536.4 ± 18.1 af y^{-1} for mesquite near the Borrego Sink and 145.7 ± 11.4 af y^{-1} at the Clark Dry Lake comparison site (Table 3). It should be noted that estimates of mesquite acreage come from image classification performed on 2016 satellite imagery but these values were treated as a static value across 2019 to 2023 water years in lieu of more recent estimates.

As a test of the accuracy of OpenET for calculating ET_{gw} by vegetation in this arid climate, we compared the remote sensing product to a known value of groundwater pumped by an agricultural user. We selected this agricultural user due to the presence of healthy citrus orchards and a constrained geographic area of 400 acres across three parcels (Fig. 6), which made it simpler to scale our estimates. The Water Year 2022 Annual Report indicates 1,651.72 af of groundwater were pumped by this user in the 2022 water year (West Yost, 2023; p. 47, Table 13) and OpenET estimated 1,396 af of groundwater use (see Appendix C for methods). Hence, OpenET estimated ET_{gw} of this agricultural user at 84.5% of estimates from metered, pumped groundwater. This estimate is reasonable considering likely return flows from irrigation inefficiency and soil evaporation, which provides us with confidence that our ET_{gw} estimates of mesquite bosque are conservative.

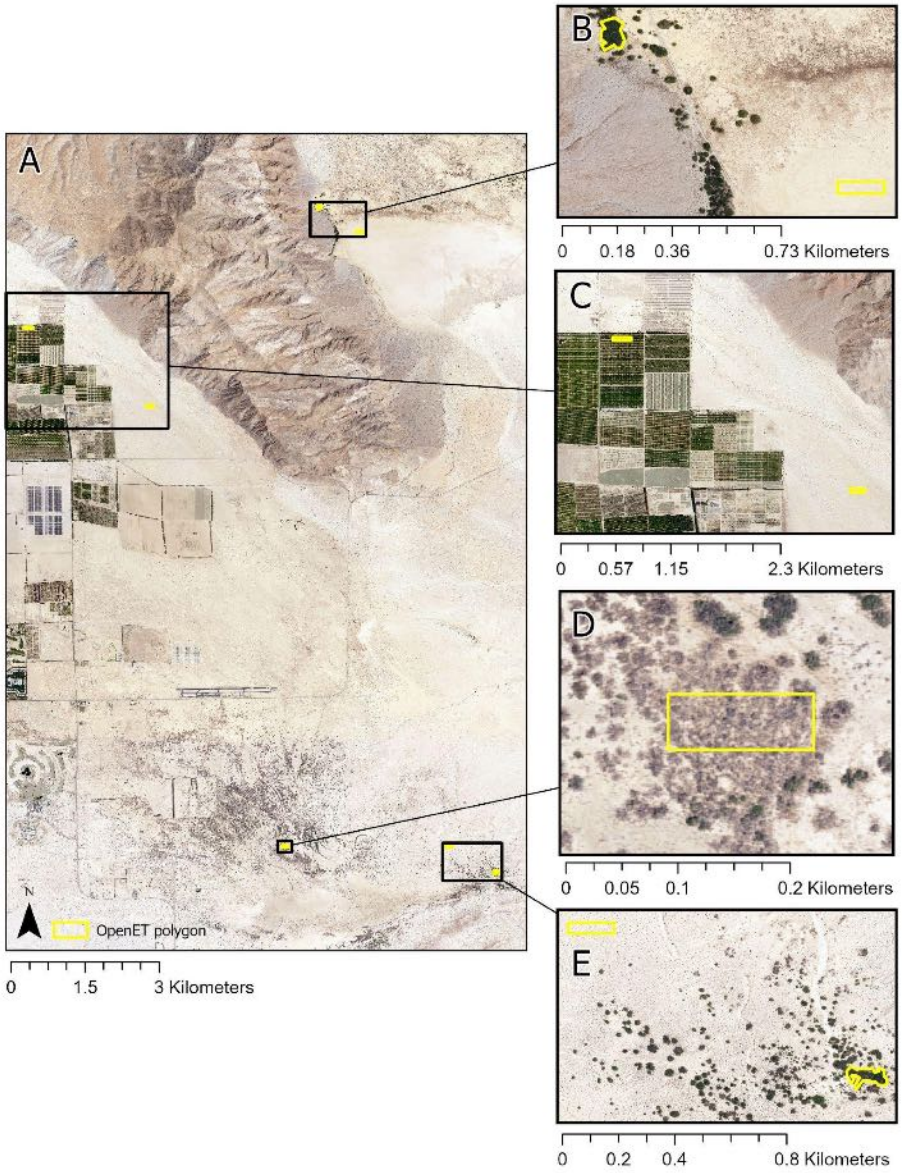


Figure 6. Map of the patches across which OpenET was run (A). The yellow polygons indicate the patches used to calculate actual ET in OpenET. Inset B is the Clark Dry Lake comparison; inset C is the agriculture example; inset D is the dead mesquite near the Borrego Sink; and inset E shows the live mesquite patch and the non-target vegetation patch near the Borrego Sink). See methods in Appendix C. Base imagery from the National Agriculture Imagery Program (NAIP) taken 22 - 23 April 2016.

Table 3. Scaled estimates of mesquite groundwater transpiration (ET_{gw}, that beyond what would be supported by localized precipitation) in acre-feet (af) near the Borrego Sink in Borrego Springs and Clark Dry Lake which have an acreage of 350.1 and 86.2, respectively.

		Mesquite Groundwater Transpiration
Site	**Water Year**	**Surplus ET (af)**
Borrego Springs	2019	532.15
	2020	556.66
	2021	525.15
	2022	553.16
	2023	514.65
Clark Dry Lake	2019	146.54
	2020	138.78
	2021	156.02
	2022	156.88
	2023	130.16

4. Isotopic analyses document groundwater use at Clark Dry Lake

While we are still waiting for the isotopic analysis from several of our sampling campaigns and locations, we can interpret the complete April 2023 data set from Clark Dry Lake. These data show that surface water alone cannot explain the isotopic signature of mesquite tissue water (Fig. 6 and 7; (Appendix D for methods). We include this data to illustrate how we will use similar data from the Borrego Sink.

We walk through interpretation of these data in Fig. 6, which details how data should behave given the expectation that mesquite-tissue water was supplied by soil water (surface water) alone, well water (groundwater) alone, or a combination of the two (mixed water source). Then we demonstrate that the isotopic signature of mesquite tissue water from Clark Dry Lake indicates a mixed water source (Fig. 7).

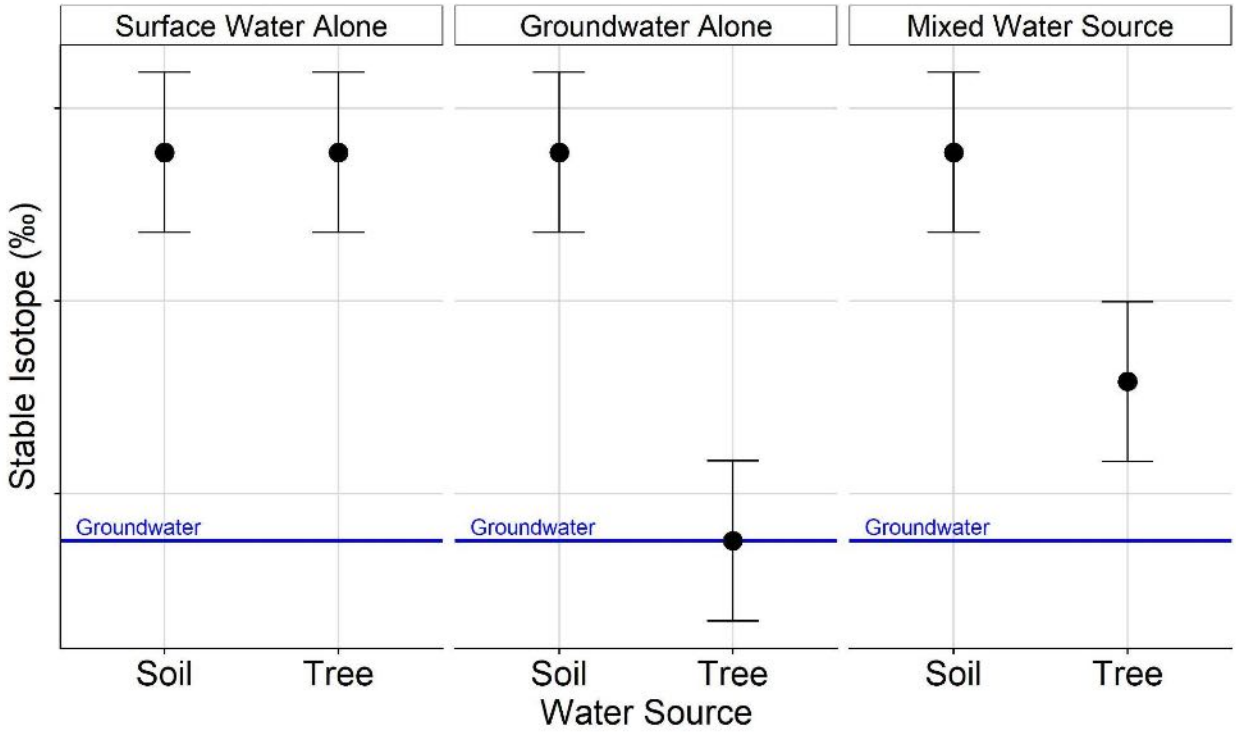


Figure 6. Conceptual representation of the isotope signatures found under hypothetically different water-use contexts. Under the *Surface Water Alone* scenario, there is complete overlap of the isotope composition of the soil water and tree tissue water. The variance in the tree tissue water data is equivalent to, or can be explained by the variance in the soil water signal. In the *Groundwater Alone* scenario (not expected but included here as a comparison), there is no overlap between the soil water isotope composition data and the tree isotopic composition data; there is only overlap with the groundwater isotope composition. In the *Mixed Water Source* scenario, the tree tissue isotopic composition is intermediate between the soil water and groundwater isotopic composition. This can be conceptualized by the notion that the surface water signal is diluted by the groundwater signal in the tree tissue. The groundwater (blue) isotope composition is represented as a line because of the low variation expected in groundwater at a single time point within a localized area. The soil and tree tissue water are represented by the mean (point) and standard deviation (error bars) because we expect variation to occur on the time and spatial scales associated with our sampling due to rainfall infiltration, percolation to depth, and soil water evaporation.

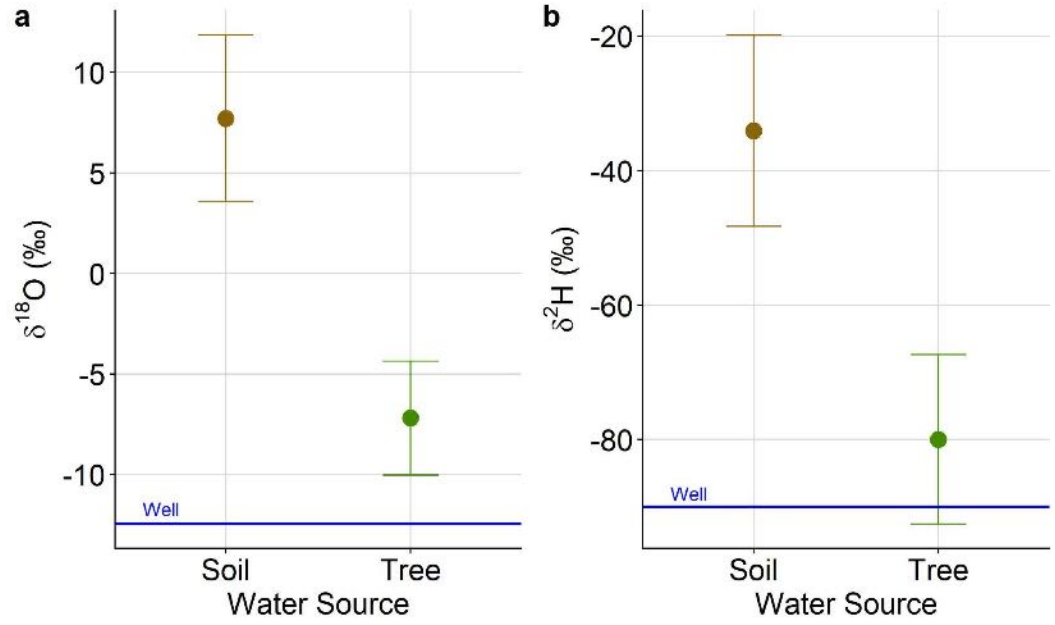


Figure 7. $\delta^{18}O$ (a) and $\delta^{2}H$ (b) of the soil water (brown), tree tissue water (green), and well water (blue) at Clark Dry Lake. The well water is a line because the value comes from a single well (two replicates that were averaged; range: -12.5 to -12.4). These data indicate a mixed water source for mesquite. The soil and tree tissue water are represented by the mean (point) and standard deviation (error bars).

We ran simple, two end-member mixing models with the average $\delta^{18}O$ or $\delta^{2}H$ of the Clark Dry Lake groundwater value as one end-member, and the average soil profile value as the other end member (Post 2002). This approach assumes that soil moisture contributes uniformly as a source across 0-130 cm soil depth to patterns of root uptake, which is a conservative estimate for determining the end-member. Equation 2 below is an example of how this mixing model calculates the proportion of groundwater in mesquite tissue using average $\delta^{18}O$ data from all 12 trees at Clark Dry Lake,the Clark Dry Lake well water, and the average soil profile values from Clark Dry Lake.

$$\text{Proportion of groundwater in mesquite tissue} = \frac{\delta^{18}O_{Tree} - \delta^{18}O_{Soil}}{\delta^{18}O_{Well} - \delta^{18}O_{Soil}} \quad (2)$$

$$\text{Proportion of groundwater in mesquite tissue} = \frac{-7.2 - 7.7}{-12.5 - 7.7}$$

$$\text{Proportion of groundwater in mesquite tissue} = 0.74$$

$$\text{Percentage of groundwater in mesquite tissue} = 74\%$$

The $\delta^{18}O$ and $\delta^{2}H$ results indicate that 74% and 82% of the water in mesquite tissues at Clark Dry Lake, respectively, result from the groundwater isotopic signature.

Conclusions and Next Steps

Our project results to date indicate high likelihood of GDEs in the Borrego Springs Subbasin, supported by multiple independent lines of evidence. Our advancements in mesquite bosque mapping using high resolution imagery from 2016 resulted in the identification of 1,800 acres of mesquite bosque near the Borrego Sink. The remote sensing analyses and estimates of groundwater transpired from OpenET indicate that mesquite in this area actively use groundwater at a scale relevant to the basin water budget. Additionally, we have provided the conceptual framework for interpreting isotope results and preliminary results from Clark Dry Lake, with results from Borrego Springs forthcoming. Looking forward, our focus will be on refining our remote sensing analyses, collecting additional isotope data at our established sites, monitoring flora and fauna, and measuring actual evapotranspiration *in situ*. Three major initiatives in the coming year will be (1) wildlife camera internships, (2) expanded spatial sampling of isotopes to enhance our understanding of the spatial extent of GDE in the Subbasin, and (3) deployment of micrometeorological sensors to narrow our estimate of mesquite transpired groundwater at our sites near the Borrego Sink and at our comparison site at Clark Dry Lake.

References

Eamus, D., Zolfaghar, S., Villalobos-Vega, R., Cleverly, J., and Huete, A. (2015). Groundwater-dependent ecosystems: recent insights from satellite and field-based studies. *Hydrology and Earth System Science, 19*, 4229–4256.

Eamus, D., Fu, B., Springer, A. E., & Stevens, L. E. (2016). Groundwater dependent ecosystems: classification, identification techniques and threats. *Integrated groundwater management: concepts, approaches and challenges*, 313-346.

Melton, F.S., Huntington, J., Grimm, R., Herring, J., Hall, M., Rollison, D., Erickson, T., Allen, R., Anderson, M., Fisher, J.B. and Kilic, A. (2022). OpenET: Filling a critical data gap in water management for the western United States. *JAWRA Journal of the American Water Resources Association*, *58*(6), 971-994.

National Agriculture Imagery Program (NAIP) Digital Object Identifier (DOI) number: /10.5066/F7QN651G

Post, D. M. (2002). Using stable isotopes to estimate trophic position: Models, methods, and assumptions. *Ecology*, *83*(3), 703–718. https://doi.org/10.1890/0012-9658(2002)083[0703:USITET]2.0.CO;2

San Diego Geographic Information Source (SanGIS). (2022). "ECO_VEGETATION_CN" Layer. Regional Vegetation to illustrate the vegetation communities and disturbed areas throughout San Diego County. Available at https://gis-sangis1.hub.arcgis.com/pages/download-data. Version: 13 October 2022.

UCI (2023). Technical Memorandum: Review of Technical Work That Supported Groundwater Dependent Ecosystems (GDE) Conclusions in the Borrego Subbasin Groundwater Management Plan. Available at https://anzaborrego.ucnrs.org/wp-content/uploads/2024/02/Technical.memorandum.3.25.2023.pdf

West Yost (2023). Water Year 2022 Annual Report for the Borrego Springs Subbasin. Project manager: Samantha Adams. QA/QC Review: Andy Malone. Available at https://borregospringswatermaster.com/wp-content/uploads/2023/03/R-940-Water-Year-2022-Annual-Report-230227-ch.pdf

APPENDICES

Appendix A.

Image classification

Methods

To identify the coverage of mesquite within our study area we used object-based supervised classification in ArcGIS Pro (v. 3.1.0) with the Support Vector Machine (SVM) as our supervised classification approach. Supervised image classification involves the researchers creating training samples which the software then learns from in order to classify the entire image into set categories (Table A1). We used the default settings for SVM within ArcGIS. We classified 0.7 m resolution National Agriculture Imagery Program imagery (NAIP) visualized in the near infrared as this provided greater contrast between the mesquite and perennial shrubs. The NAIP imagery came from 22 and 23 April 2016 and was mosaicked in Google Earth Engine. This year was selected because it was the closest year to SGMA implementation (2015) that contained high quality imagery when plants were active.

We conducted the supervised image classification for our two primary sites separately. In the Borrego Springs Subbasin, we used the Palm Canyon Drive and Borrego Valley Road as our north and west bounds, respectively. To the south and east, we used the extent of mesquite within the Borrego Springs Subbasin as our bounds (Fig. A1). At Clark Dry Lake, we included the expanse between the feet of the two mountain ranges bounding the lake to the east and west (Fig. A1). Training samples took the form of polygons (Table A1). There were some spots in the Clark Dry Lake area that had been mapped by the County of San Diego (SanGIS, 2022) as mesquite bosque that were challenging to determine from aerial imagery whether the vegetation was mesquite or creosote bush, so our partners at the San Diego Natural History Museum investigated on the ground. After classification, classes other than Live Mesquite were reclassified as Barren in order to simplify validation, as only the Live Mesquite category was of interest. For validation, we used 100 random assessment points per category (equal stratification for Live Mesquite and Barren) for each primary site. We report user's accuracy, producer's accuracy, overall accuracy, and kappa (Congalton 1991). User's accuracy indicates the probability that a classified object actually represents that category according to the validation data. Overall accuracy is the percentage of true positives. Kappa evaluates the performance of the classification compared to random assignment where values closer to one indicate the classification is better than random assignment (Viera & Garrett 2005).



Figure A1. The areas across which image classification was performed.

Table A1. The categories and cover of training samples at each primary site.

Site	Category	No. of Samples	% of Pixels
Borrego Springs	Barren	47	42.92
	Dead Mesquite	86	1.71
	Live Mesquite	71	2.54
	Shrubland	33	52.73
	Shadow	15	0.1
Clark Dry Lake	Barren	9	91.65
	Live Mesquite	18	0.2
	Shrubland	8	8.13
	Shadow	3	0.02

The Borrego Springs supervised image classification had an overall accuracy of 96% and the Clark Dry Lake supervised image classification had an overall accuracy of 95% (Table A2). The kappa coefficient for the Borrego Springs supervised image classification was 0.92 and the kappa coefficient for the Clark Dry Lake supervised image classification was 0.9 (Table A2).

Table A2. Results of the accuracy assessment. Columns indicate what the object actually was based on validation data and the rows represent what the pixel was classified as.

Site		Bareground	Live Mesquite	User's Accuracy (%)
Borrego Springs	Bareground	99	1	99
	Live Mesquite	7	93	93
	Producer's Accuracy (%)	93.4	98.9	**Overall Accuracy** = 96% **Kappa** = 0.92
Clark Dry Lake		Bareground	Live Mesquite	User's Accuracy (%)
	Bareground	100	0	100
	Live Mesquite	10	90	90
	Producer's Accuracy (%)	90	100	**Overall Accuracy** = 95% **Kappa** = 0.9

Mapping of the mesquite bosque

Methods

The image classification was used alongside on the ground field observations to redraw the boundaries of mesquite bosque in the Borrego Sink area and Clark Dry Lake. These new boundaries were compared to those from a map created by the City and County of San Diego as well as the San Diego Association of Governments in 1995 which characterizes vegetation communities according to the Holland system (Holland 1986, SanGIS 2022).

To redraw the boundaries of the mesquite bosque we first selected only the polygons produced during image classification with an area greater than 5 m^2 in order to minimize the presence of shrubs which may have been inaccurately classified. We next created a 5 m buffer around the resultant polygons.

Then we aggregated the resultant polygons that were within 10 m from each other to include only polygons with a minimum size of 400 m^2 after aggregation and a minimum hole size of 1000 m^2. The buffering and aggregating steps were done to ensure we mapped a mesquite bosque ecosystem rather than individual, isolated mesquite trees. Next, to produce polygons with a simplified shape, we simplified the polygons with the "Retain Critical Bends (Wang-Müller)" simplification algorithm with a 25 m simplification tolerance and a minimum area of 1000 m^2. We then eliminated polygon holes smaller than 50,000 m^2 and used the dissolve tool to merge all overlapping polygons. Finally, we aggregated polygons within 50 m of each other in order to better capture the mesquite bosque habitat, which includes interstitial space and associated understory vegetation in addition to live mesquite trees. To quantitatively assess the resultant mesquite bosque habitat area, we used the vegetative alliances assigned by the Manual of California Vegetation (Sawyer et al. 2009), which is distributed by the California Native Plant Society and the California Department of Fish and Wildlife and employs a quantitative assignment system adopted by state and federal agencies. The mesquite thickets alliance (also known as the *Prosopis glandulosa - Prosopis velutina - Prosopis pubescens* Woodland Alliance) is equivalent to Holland's mesquite bosque grouping originally used to map the mesquite bosque in 1995 and the most stringent membership qualifications stipulate an absolute cover of mesquite greater than 2% (Sawyer et al. 2009). To ensure our map met this qualification we selected the image classification polygons found only within the map area and then divided the total area of those polygons by the total area of the mapped mesquite bosque. For the Borrego Springs map, we found an absolute cover of 16.6% mesquite by area. For the Clark Dry Lake, we found an absolute cover of 36.4% mesquite by area. Hence, our mapping effort is conservative as it includes land surface with cover considerably higher than the minimum threshold of 2% identified by the Manual of California Vegetation definition for the mesquite thickets alliance (Sawyer et al. 2009).

Appendix B.

Remote Sensing Approaches

Normalized Difference Vegetation Index (NDVI)

In remote sensing, vegetation health, density, and greenness is often measured with Normalized Difference Vegetation Index (NDVI). NDVI is derived from satellite and aerial imagery and is calculated using the near-infrared (NIR) and red bands of the electromagnetic spectrum captured by remote sensors. The formula for NDVI is:

$$NDVI = \frac{NIR - RED}{NIR + RED}$$

The relationship between NDVI and vegetation arises from the fact that healthy vegetation reflects a large amount of near-infrared light due to chlorophyll's unique absorption properties, and also absorbs most of the visible red light for photosynthesis. The values of NDVI range from -1 to 1, with higher values between 0.5 and 1 indicating denser, healthy vegetation. Values between 0.2 and 0.5 indicate moderate density-vegetation, that may not be as lush or healthy as vegetation with higher values. Values between 0-0.2 typically indicate low-density, sparse, or stressed vegetation. Values below zero indicate the absence of live vegetation, such as bare soil, concrete, or water.

We can use NDVI and the "green island" theory to systematically detect subtle differences in vegetation in response to ecosystem water availability. This method has proven useful in arid and semi-arid regions where groundwater plays a critical role in supporting ecosystems, and is a recommended approach in GDE literature (Eamus et al. 2015).

Supporting Information for Remote Sensing Approach 1

Background

Plants require water for their survival. In the absence of rainfall and adequate soil moisture during the growing season, plants are unable to photosynthesize and may enter a phase of senescence or dormancy. This leads to consistent (*i.e.* monotonic) decreases in NDVI throughout dry periods as the amount of vegetation and green leaves decrease over time. However, when plants have access to groundwater during the growing season, they can continue to thrive even during prolonged dry spells, thus maintaining or increasing their NDVI while remaining physiologically active and growing new leaves despite the dry conditions (Eamus et al. 2015; Gou et al. 2015).

To explore this behavior, we can analyze remotely sensed NDVI data collected during dry periods within the growing season (we illustrate May 21 through June 20, 2023, corresponding to days 50-80

of the summer drought as an example). By calculating Mann-Kendall's tau for each pixel across this dry period, we can assess how NDVI values change over time. We anticipate that the non-GDE will exhibit negative tau values, indicating a consistent decrease in NDVI throughout the dry period as the vegetation declines without access to water. In contrast, the GDEs may demonstrate positive or near-zero tau values, indicating either an increase or stability in NDVI over the dry period due to the availability of groundwater to support plant growth.

Description of Monotonic Trends and Mann Kendall's tau

Monotonic trends refer to a consistent directional change in a dataset over time, characterized by either consistent increase or decrease without significant fluctuations. Mann-Kendall's tau is a statistical test employed for detecting such monotonic trends in a dataset (Kendall 1948). Kendall's tau quantifies the strength and direction of the monotonic trend: a positive tau value signifies an increasing monotonic trend, whereas a negative value indicates a decreasing trend. Tau values near zero indicate the absence of a monotonic trend meaning NDVI either fluctuated or remained stable over time.

Assumption

GDE should have tau values ≥ 0, meaning it maintained or increased NDVI across the dry period. Non-GDEs should have tau values < 0, meaning it decreased in NDVI across the dry period.

Methods

To identify relevant dry period dates within the mesquite growing season (March through November) for Approaches 1 and 2, we analyzed PRISM daily climate data (PRISM Climate Group, 2024). To validate the PRISM rainfall data, we cross-referenced it with rainfall and surface soil moisture data collected from weather stations in Borrego Springs (https://anzaborrego.ucnrs.org/weather/). We identified an extended dry period in 2023 spanning 121 consecutive rain-free days from March 31- July 30, 2023.

For Approach 1, we focus on days 50-80 of the 2023 drought (May 21 - June 20, 2023) to isolate a time period within the mesquite growing season characterized by consistently dry surface soils. We then filtered Sentinel 10 m resolution satellite imagery for the selected dry period dates for each area of interest (AOI). Next, we calculated NDVI for each image available and masked all pixels with NDVI <0.1 during the dry period to eliminate areas with no live vegetation from the analysis. We then computed Mann Kendall's tau across the dry period for each pixel.

AOIs:

Potential GDE: Borrego Springs Mesquite Habitat Polygons (BS)
Known GDE: Clark Dry Lake Mesquite Habitat Polygons (CDL)
Non-GDE: A polygon of non-GDE community near Coyote Creek (non-GDE)

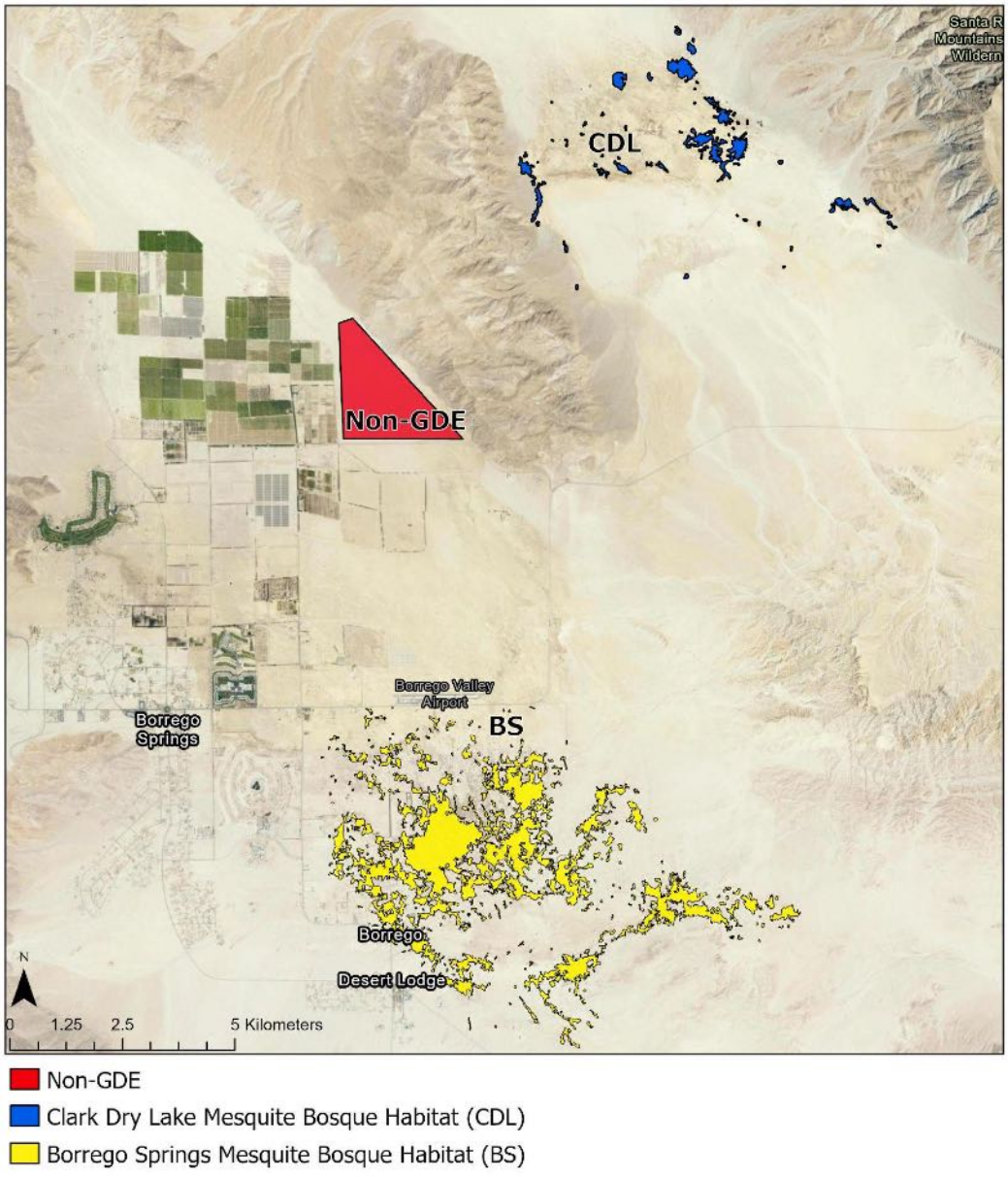


Figure B1. Map of the areas of interest (AOIs) used in Approach 1, including the Non-GDE, the known GDE Clark Dry Lake (CDL), and the potential GDE Borrego Springs (BS) polygons used in the remote sensing approaches.

Results

The maximum tau value for the non-GDE was -0.2, indicating that all non-GDE pixels demonstrated consistent NDVI decreases, meaning that no plant growth was observed across the dry period (Table B1). Conversely, at Clark Dry Lake, 25% of mesquite bosque pixels demonstrated tau values greater than 0, indicating that NDVI increased or remained stable across the dry period, indicative of plant growth or maintenance supported by groundwater use (Table B2). In Borrego Springs, 22% of mesquite bosque pixels had tau values greater than 0, indicating that a significant portion of this area likely qualifies as a GDE (Figure B2, Table B2).

Table B1. Summary of maximum tau values found in each area of interest (AOI).

Area of Interest (AOI)	**Maximum tau value**	**Interpretation**
Non-GDE	-0.2	Weak NDVI decrease across dry period
Clark Dry Lake	0.9	Strong NDVI increase across dry period
Borrego Springs	1.0	Strong NDVI increase across dry period

Table B2. Summary of maximum tau values found in each area of interest (AOI).

Area of Interest (AOI)	**Percent of Pixels with tau ≥ 0.0**	**Interpretation**
Non-GDE	0 %	No pixels within AOI are likely to be GDE
Clark Dry Lake	25 %	25% of pixels are highly likely GDE
Borrego Springs	22 %	22% of pixels are highly likely GDE

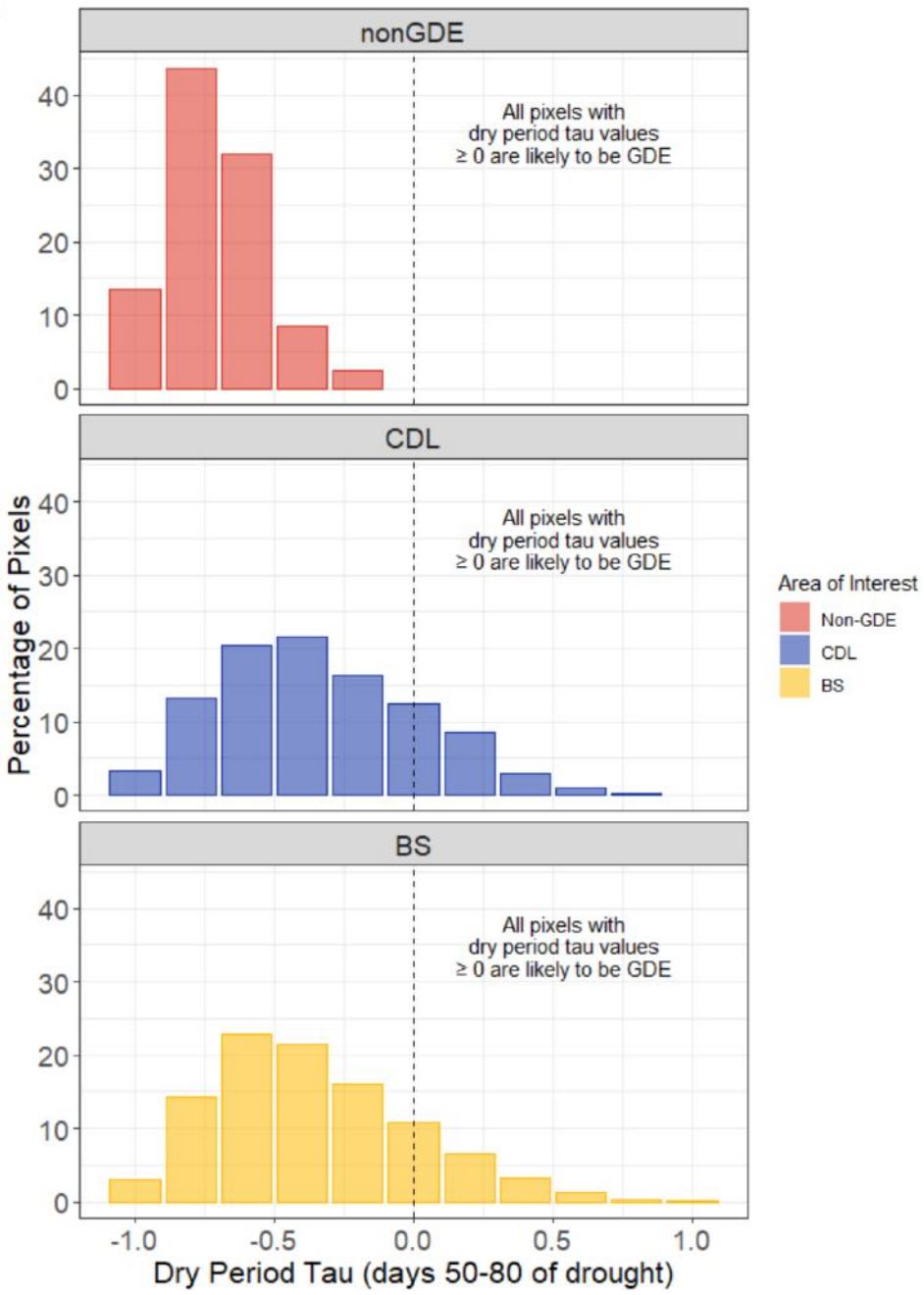


Figure B2. The percentage of pixels and the Mann Kendall tau value found between May 21- June 20, 2023 (days 50-80 of drought) for each area of interest. Pixels with tau values ≥ 0 indicate that the NDVI increased or remained stable across the dry period, which indicates plant physiological activity that could only be supported by reliable access to groundwater. The Non-GDE had 0% of pixels with tau ≥ 0; CDL had 25% of pixels with tau ≥ 0; BS had 22% of pixels with tau ≥ 0.

Supporting Information for Remote Sensing Approach 2

Background

Plants rely on water for their survival, as it is essential for photosynthesis. In the absence of rainfall and soil moisture, plants cannot photosynthesize and may enter a phase of senescence or dormancy. When low soil moisture coincides with high temperatures for an extended period, plants experience heat stress, wilting, and dormancy or death. Consequently, NDVI values may plummet to near-zero after prolonged dry spells, signifying the loss of live vegetation. However, when plants have access to groundwater, they can continue to survive throughout prolonged dry spells, thus maintaining high NDVI (Eamus et al 2015; Gou et al. 2015).

To investigate this behavior, we can analyze remotely sensed NDVI data collected during extreme dry periods within the growing season (we illustrate June 20-July 30, 2023, corresponding to days 80-120 of the summer drought as an example). During this period, the average daily maximum temperature in Borrego Springs was 106°F (41.1°C). By calculating the maximum NDVI for each pixel during this extreme dry period, we can assess the amount of live, photosynthetically active vegetation on the landscape. We expect that the non-GDE will exhibit low NDVI values, indicating an absence of live vegetation across the landscape. Conversely, GDEs may display higher NDVI values, indicating the persistence of live vegetation despite severe heat and dry soil.

Description of maximum NDVI

The maximum NDVI for each pixel is derived by identifying the highest NDVI value recorded within a specified time period. The maximum NDVI serves as a proxy for the peak vegetation greenness observed during the period, enabling us to assess the amount of live vegetation present on the landscape. Areas exhibiting maximum NDVI values close to 1 are indicative of dense, live vegetation, while values closer to 0 may signify sparse or inactive vegetation.

Assumption

GDE should have higher NDVI across extreme dry periods than non-GDE due to the presence of live vegetation with access to groundwater.

Methods

For Approach 2, we focus on days 80-120 of the 2023 drought (June 20-July 30, 2023) to isolate a time period within the mesquite growing season characterized by consistently dry surface soils and high temperatures. We then filtered Sentinel 10 m resolution satellite imagery for the selected dry period

dates for each AOI (see figure B1). Next, we calculated NDVI for each image available and computed the maximum NDVI for each pixel across the dry period.

AOIs:

Potential GDE: Borrego Springs Mesquite Habitat Polygons (BS)

Known GDE: Clark Dry Lake Mesquite Habitat Polygons (CDL)

Non-GDE: A polygon of non-GDE community near Coyote Creek (non-GDE)

Results

The maximum dry period NDVI value for the non-GDE was 0.18, indicating that all non-GDE pixels had low NDVI across the dry period, meaning that little to no live vegetation was present (Table B3). Conversely, at Clark Dry Lake, 60% of mesquite bosque pixels demonstrated maximum dry period NDVI values greater than 0.18, indicating that live vegetation persisted throughout the dry period, indicative of groundwater use (Table B4). In Borrego Springs, 13% of mesquite bosque pixels had maximum dry period NDVI values greater than 0.18, indicating that a significant portion of this area likely qualifies as a GDE (Figure B3, Table B4). Figure B4 provides a map of the areal extent of GDE likelihood for Approach 2, highlighting hotspots of GDE behavior across the BS mesquite bosque.

Table B3. Summary of maximum dry period NDVI values found in each area of interest (AOI).

Area of Interest (AOI)	**Maximum dry period NDVI**	**Interpretation**
Non-GDE	0.18	Little to no live vegetation
Clark Dry Lake	0.87	Dense live vegetation
Borrego Springs	0.85	Dense live vegetation

Table B4. Summary of maximum dry period NDVI values found in each area of interest (AOI).

Area of Interest (AOI)	**Percent of Pixels with max NDVI > 0.18**	**Interpretation**
Non-GDE	0 %	No pixels within AOI are likely to be GDE
Clark Dry Lake	60 %	60% of pixels are highly likely GDE
Borrego Springs	13 %	13% of pixels are highly likely GDE

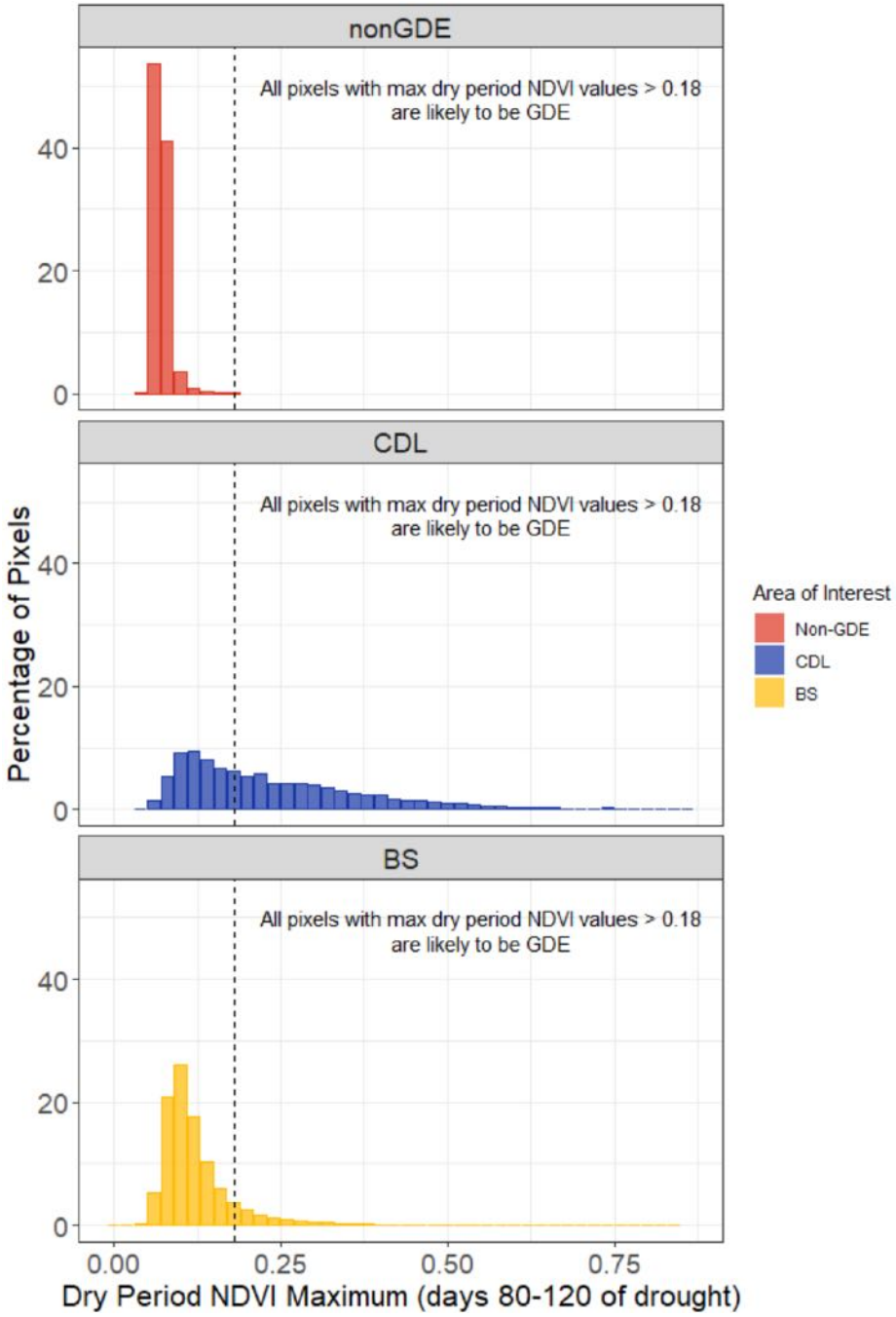


Figure B3. The percentage of pixels and the dry period maximum NDVI for each area of interest. Pixels with maximum NDVI values >0.18 indicate live vegetation that could only persist during extended dry periods due to groundwater access. The Non-GDE had 0% of pixels with maximum NDVI >0.18; CDL had 60% of pixels with maximum NDVI >0.18; BS had 13% of pixels with maximum NDVI >0.18.

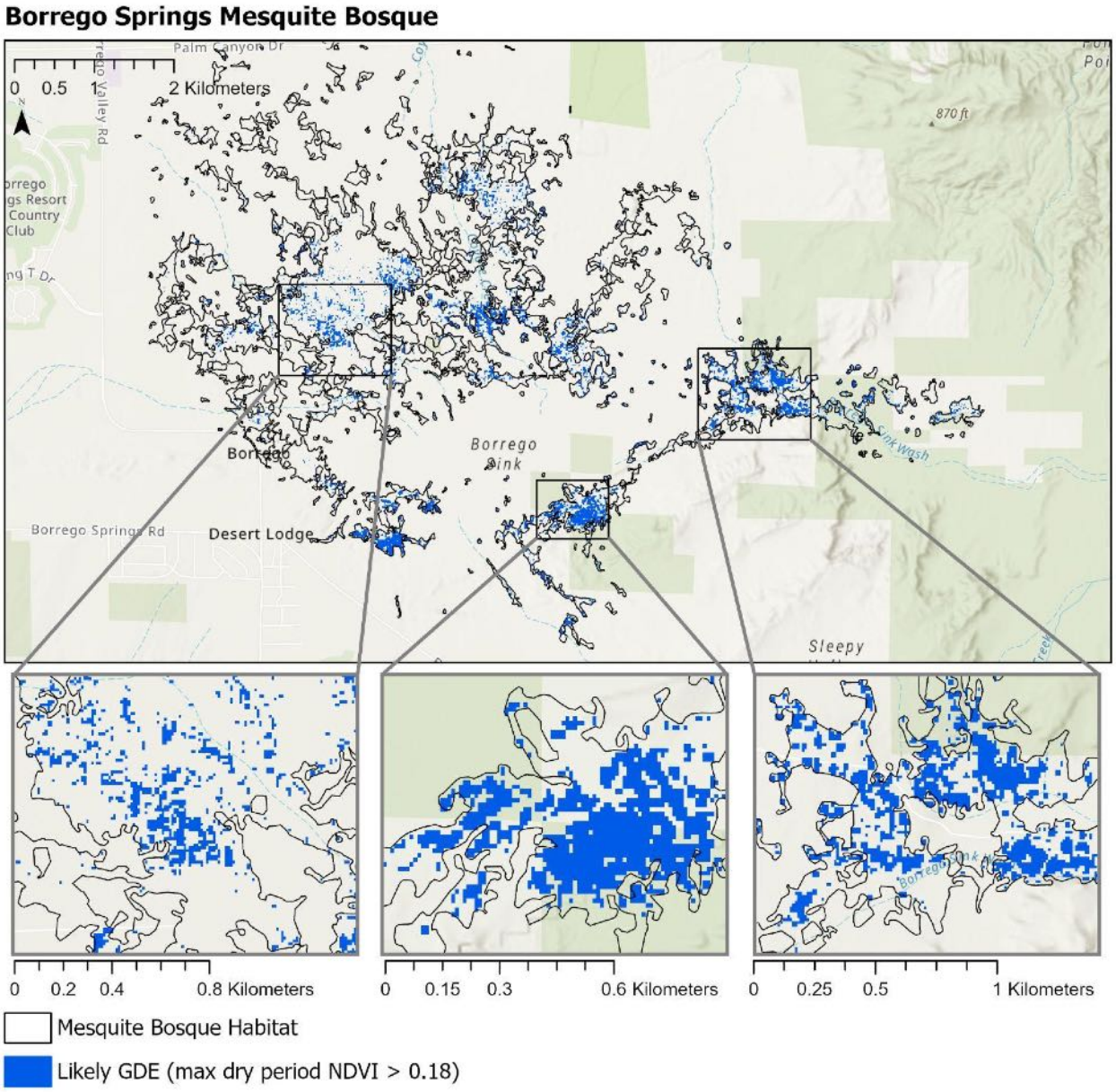


Figure B4. Map of the spatial extent of GDE behavior identified in Approach 2, which analyzes the maximum NDVI across an extended dry period in 2023 for the Borrego Springs mesquite bosque. Areas shown in blue indicate vegetation that has NDVI values greater than 0.18 across extended dry periods, indicating live vegetation that is likely supported by groundwater access.

Supporting Information for Remote Sensing Approach 3

Background

Plants with greater access to water typically exhibit higher levels of photosynthetic activity. Cumulative annual NDVI serves as a reliable indicator of Gross Primary Productivity (GPP), reflecting the overall photosynthetic activity of vegetation throughout the entire year (Ricotta et al. 1999). The continuous availability of groundwater enables GDEs to maintain active photosynthesis during dry periods when non-GDEs may experience water stress and reduced productivity. Consequently, GDEs tend to display higher GPP and thus higher cumulative NDVI values (Eamus et al 2015).

To explore this behavior, we can examine cumulative annual NDVI across the water year as a proxy for GPP (we illustrate the 2023 water year, from October 1, 2022 to September 30, 2023 as an example). By calculating cumulative annual NDVI, we can assess the relative productivity of GDEs compared to non-GDEs. We anticipate that the non-GDE will exhibit low cumulative annual NDVI, indicating low photosynthetic activity throughout the majority of the year. In contrast, the GDEs may demonstrate high cumulative annual NDVI, indicating greater vegetation productivity and drought resilience throughout the year.

Description of cumulative annual NDVI

Cumulative annual NDVI is derived by summing the NDVI values for each pixel over the year, and is used as a measure of the total green biomass production, or GPP. This cumulative metric captures the integrated effects of various environmental factors on vegetation growth, including groundwater access, precipitation, soil moisture, and temperature. Higher cumulative NDVI values signify greater photosynthetic activity throughout the year, indicative of robust vegetation growth under favorable environmental conditions. Conversely, lower cumulative NDVI values suggest diminished photosynthetic activity, reflective of less favorable or challenging environmental conditions throughout the year.

Assumption

GDE should have higher cumulative NDVI than non-GDE due to the potential to accumulate greater plant biomass throughout the year due to access to groundwater.

Methods

For Approach 3, we focus on the 2023 water year (October 1, 2022 to September 30, 2023) to evaluate mesquite productivity over the course of the entire year. We filtered Sentinel 10 m resolution satellite imagery for the selected dates for each AOI (see Figure B1). Next, we calculated NDVI for each image available and then summed all NDVI values from each pixel over the time frame to calculate the cumulative 2023 NDVI.

AOIs:

Potential GDE: Borrego Springs Mesquite Habitat Polygons (BS)

Known GDE: Clark Dry Lake Mesquite Habitat Polygons (CDL)

Non-GDE: A polygon of non-GDE community near Coyote Creek (non-GDE)

Results

The maximum cumulative NDVI value for the non-GDE was 5.2, indicating that all non-GDE pixels had vegetation with relatively low productivity (Table B5). Conversely, at Clark Dry Lake, 65% of mesquite bosque pixels demonstrated cumulative NDVI values greater than 5.2, indicating higher vegetation productivity, likely due to the accumulation of biomass throughout the year due to groundwater access (Table B6). In Borrego Springs, 10% of mesquite bosque pixels had cumulative NDVI values greater than 5.2, indicating that a significant portion of this area likely accesses groundwater throughout the year, and is thus a GDE (Figure B5, Table B6). Figure B6 provides a map of the areal extent of GDE likelihood for Approach 3, highlighting hotspots of GDE behavior across the BS mesquite bosque.

Table B5. Summary of maximum 2023 cumulative NDVI values found in each area of interest (AOI).

Area of Interest (AOI)	**Maximum cumulative NDVI**	**Interpretation**
Non-GDE	5.2	Low productivity vegetation
Clark Dry Lake	24.7	Highly productive vegetation
Borrego Springs	19.7	Highly productive vegetation

Table B6. Summary of 2023 cumulative NDVI values found in each area of interest (AOI).

Area of Interest (AOI)	Percent of Pixels with cumulative NDVI > 5.2	Interpretation
Non-GDE	0 %	No pixels within AOI are likely to be GDE
Clark Dry Lake	65 %	65% of pixels are highly likely GDE
Borrego Springs	10 %	10% of pixels are highly likely GDE

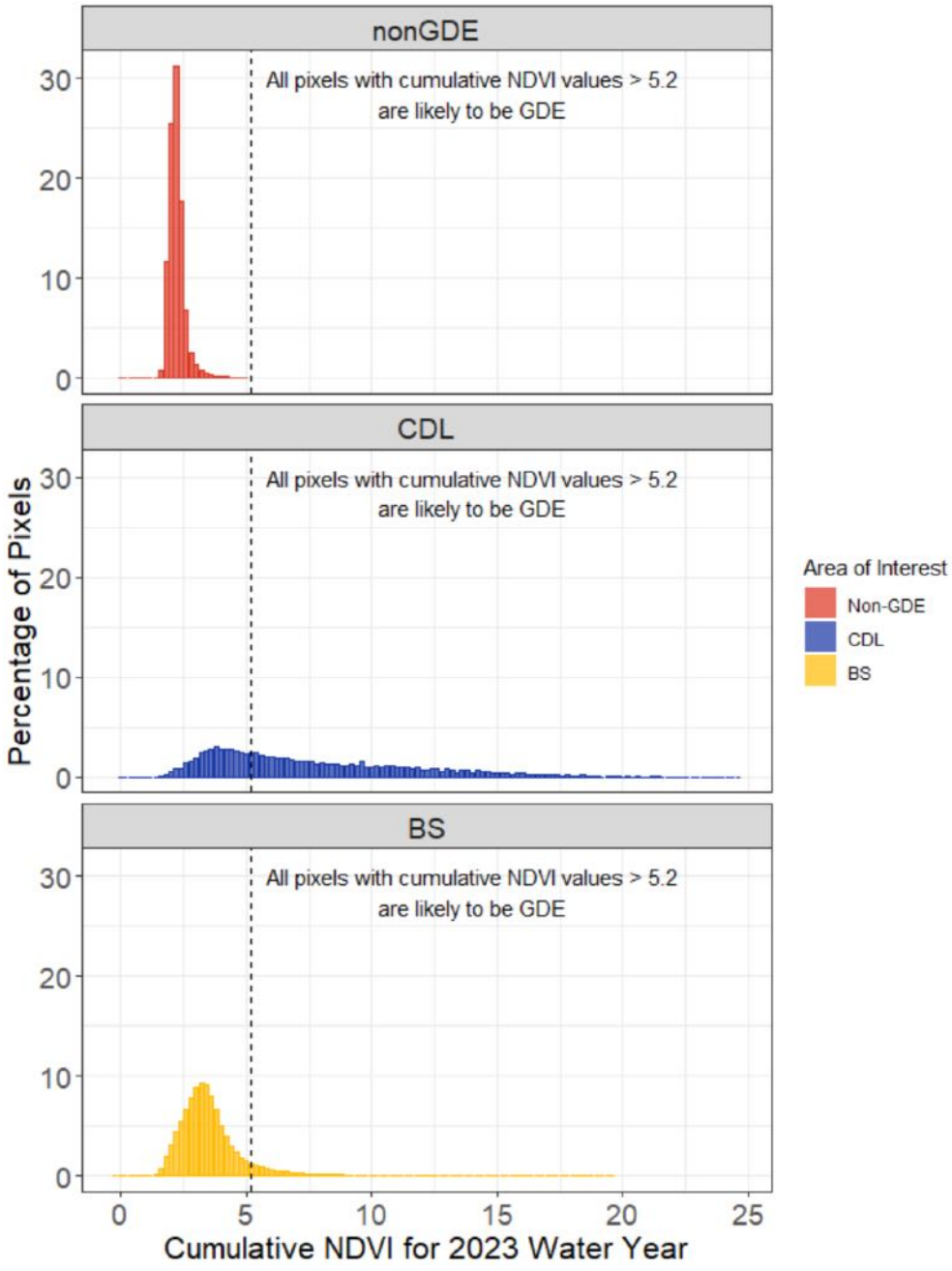


Figure B5. The percentage of pixels and the 2023 water year cumulative NDVI for each area of interest. Pixels with cumulative NDVI values >5.2 indicate highly productive vegetation that likely has access to groundwater. The Non-GDE had 0% of pixels with cumulative NDVI values >5.2; CDL had 65% of pixels with cumulative NDVI values >5.2; BS had 10% of pixels with cumulative NDVI values >5.2.

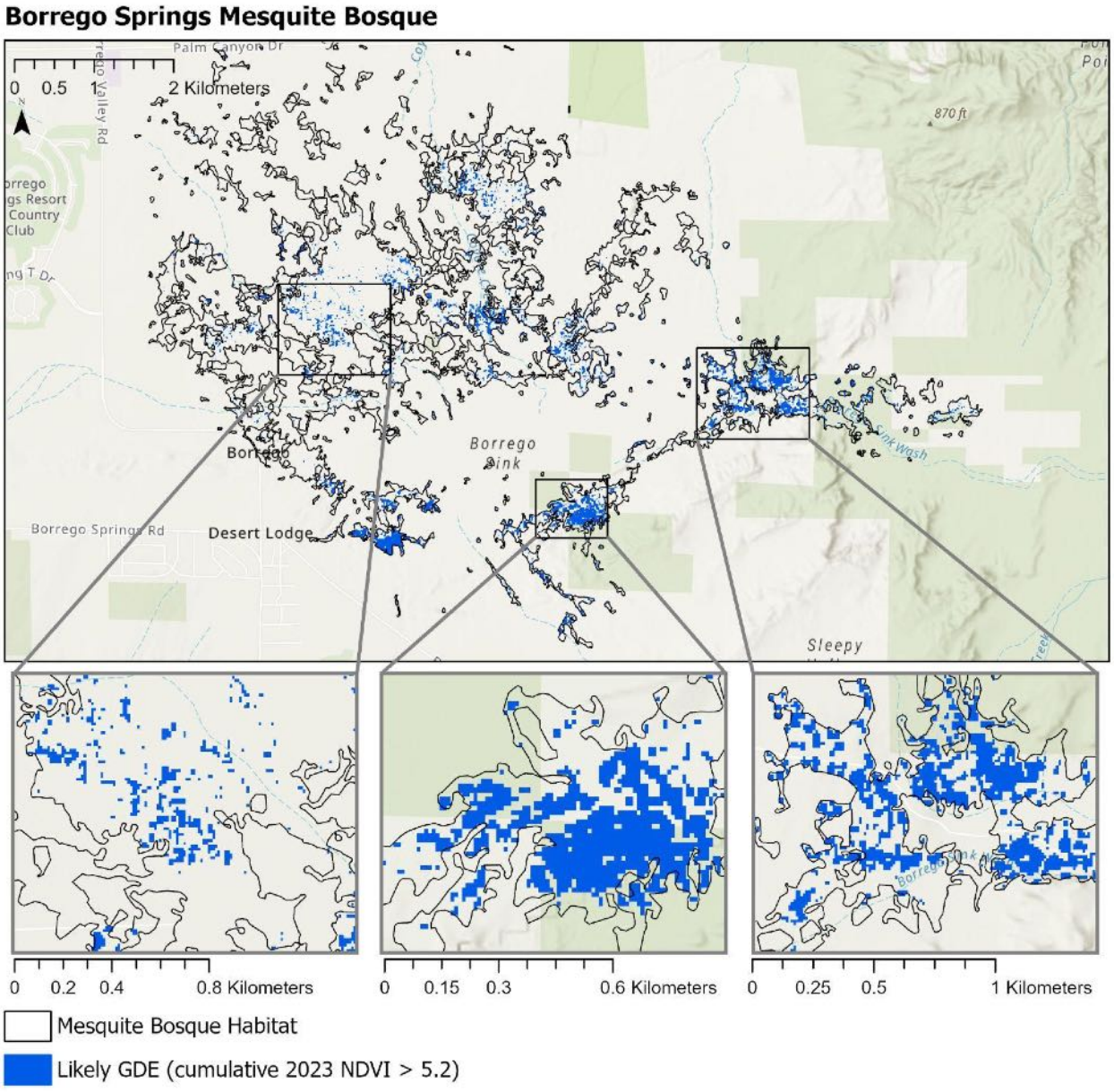


Figure B6. Map of the spatial extent of GDE behavior identified in Approach 3, which analyzes the cumulative NDVI across the 2023 water year (Oct. 1, 2022- Sep. 30, 2023) for the Borrego Springs mesquite bosque. Areas shown in blue indicate highly productive vegetation that has cumulative NDVI values greater than 5.2, and is likely supported by groundwater access.

Appendix C.

Evapotranspiration and groundwater transpiration estimates

Methods

We estimated ET from patches at three different sites–Borrego Sink area, Clark Dry Lake, and the northern agricultural area–which we then scaled up to get an estimate of acre-feet of groundwater use per year. We include an estimate of groundwater transpiration from an active agricultural site in the northern part of the Subbasin to assess the ability of remote sensing to estimate water loss to the atmosphere of a system with known groundwater use.

We subtracted precipitation from ET to get an estimate of ET that surpasses precipitation (Surplus ET), suggesting groundwater use (ET_{gw}) (Eamus et al. 2016). At each site we estimated Surplus ET from a highly vegetated patch of interest (Combined Evapotranspiration) and a nearby more-bare patch that did not include our target vegetation (representative of Soil Evaporation and Understory Transpiration). While the Soil and Understory ET estimates are higher than expected (Table C1), likely due to annual species which flourish following rain events, we can subtract this from the Combined Evapotranspiration Surplus ET values to isolate transpiration from the vegetation of interest and provide a conservative estimate of groundwater use (Transpiration from Vegetation of Interest).

Data are available from OpenET for the 2019 through 2023 water years (1 October - 30 September) (Melton et al. 2022). We used ET estimates from the Priestley Taylor-Jet Propulsion Laboratory (PT-JPL) model which was developed by Fisher et al., (2008) and is based on the Preistly Taylor equation. All patches tested are of a similar area (approximately 1.28 acres). Precipitation is provided by OpenET via Gridmet (Abatzoglou 2013). To assess the effectiveness of OpenET we scaled up a patch from an active citrus orchard in the northern agricultural area. The groundwater transpiration we derived for water year 2022 was 3.49 af per acre at this agricultural site (Table C1; Transpiration from Vegetation of Interest), which was multiplied by the acreage of the agricultural site (400 acres) to get 1,396 af of groundwater transpiration.

The estimated groundwater transpiration by the agricultural area (Table C1; Transpiration from Vegetation of Interest, Surplus: 3.42 ± 0.19) was higher than that of both the Borrego Sink and Clark Dry Lake, as expected from differences in plant density, size, and leaf area display. The Surplus ET from a patch of dead mesquite near the Borrego Sink (Table C2; 0.41 ± 0.14) had an ET value closer to that of the patches without the target vegetation (Table C1; Soil and Understory Evapotranspiration, Surplus ET: 0.056 ± 0.14) than the mesquite patches (Table C1; Combined Evapotranspiration),

which lends further credence to the transpiration values found for live mesquite. The average values for Soil and Understory Evapotranspiration ET and Precipitation were essentially equivalent (consistent with water balance theory).

UCIrvine

Table C1. Actual ET estimates in acre-feet (af) per acre for the 2019 - 2023 water years across vegetated and more bare patches.

		Combined Evapotranspiration			Soil and Understory Evapotranspiration			Groundwater Transpiration from Target Vegetation
Site	**Water Year**	**ET (af per acre)**	**Precipitation (af per acre)**	**Surplus (af per acre)**	**ET (af per acre)**	**Precipitation (af per acre)**	**Surplus (af per acre)**	**Surplus (af per acre)**
Borrego Springs	2019	2.09	0.47	1.62	0.57	0.47	0.1	1.52
	2020	2.14	0.81	1.33	0.55	0.81	-0.26	1.59
	2021	1.81	0.15	1.66	0.31	0.15	0.16	1.5
	2022	1.9	0.16	1.74	0.32	0.16	0.16	1.58
	2023	2	0.48	1.52	0.53	0.48	0.05	1.47
Clark Dry Lake	2019	2.33	0.6	1.73	0.63	0.6	0.03	1.7
	2020	2.05	0.68	1.37	0.44	0.68	-0.24	1.61
	2021	2.09	0.17	1.92	0.28	0.17	0.11	1.81
	2022	2.14	0.2	1.94	0.32	0.2	0.12	1.82
	2023	2.14	0.51	1.63	0.63	0.51	0.12	1.51
Agricultural Area	2019	4.26	0.58	3.68	0.74	0.58	0.16	3.52
	2020	4.06	0.68	3.38	0.61	0.68	-0.07	3.45
	2021	3.9	0.19	3.71	0.35	0.19	0.16	3.55
	2022	3.95	0.23	3.72	0.47	0.24	0.23	3.49
	2023	3.64	0.54	3.1	0.56	0.54	0.02	3.08

Table C2. Actual ET estimates in acre-feet (af) per acre for the 2019 - 2023 water years for a patch of dead mesquite near the Borrego Sink.

Site	Water Year	ET (af per acre)	Precipitation (af per acre)	Surplus (af per acre)
Borrego Springs	2019	0.88	0.48	0.4
	2020	1.11	0.87	0.25
	2021	0.69	0.15	0.53
	2022	0.7	0.13	0.57
	2023	0.73	0.42	0.31

UCIRVINE

Appendix D.

Isotopic analysis.

Methods

Mature mesquite twigs with expanded new leaves were selected from sunlit branches near the outer canopy. Twigs were cut approximately in 1-2 centimeter lengths, with a maximum thickness of 1.2 cm diameter. To minimize the effects of evaporation of water from the twigs, vials were quickly filled with cut twigs and capped with minimal headspace. Vials were then sealed with parafilm and were refrigerated until analysis. Twigs were collected on 10 through 12 April 2023.

Soil sampling locations for the collection of soil water were placed near tagged mesquite trees. Soil cores were extracted using a 8 cm diameter manual auger at the following depth ranges: 0-10 cm, 10-40 cm, 40-70 cm, 70-100 cm, 100-130 cm. To minimize the effects of evaporation of water from the soil, jars were quickly filled and capped with minimal headspace, sealed with parafilm, and refrigerated until analysis. Soil samples were collected from all five sites on 10 through 12 April 2023. Well water from a well owned by Anza-Borrego State Park located near Clark Dry Lake was collected on 11 April.

Water isotopes were analyzed by the University of Wyoming Stable Isotope Facility using a Temperature Conversion Elemental Analyzer coupled to a Thermo Delta Plus IRMS. We removed one outlier from the Clark Dry Lake dataset (tree 5-9) because it was greater than three standard deviations from the mean.

Results

The mean isotopic composition of mesquite at Clark Dry Lake clearly indicates groundwater use as no value of plant tissue overlaps with any soil value for both isotopes (Table D1, Fig. D1, Fig. D2).

Table D1. Average isotopic values at the comparison Clark Dry Lake site.

Site	**Mesquite Trees**		**Soil**		**Well**	
	$\delta^{18}O$	$\delta^{2}H$	$\delta^{18}O$	$\delta^{2}H$	$\delta^{18}O$	$\delta^{2}H$
Clark Dry Lake	-7.2	-80.0	7.7	-34.0	-12.5	-90

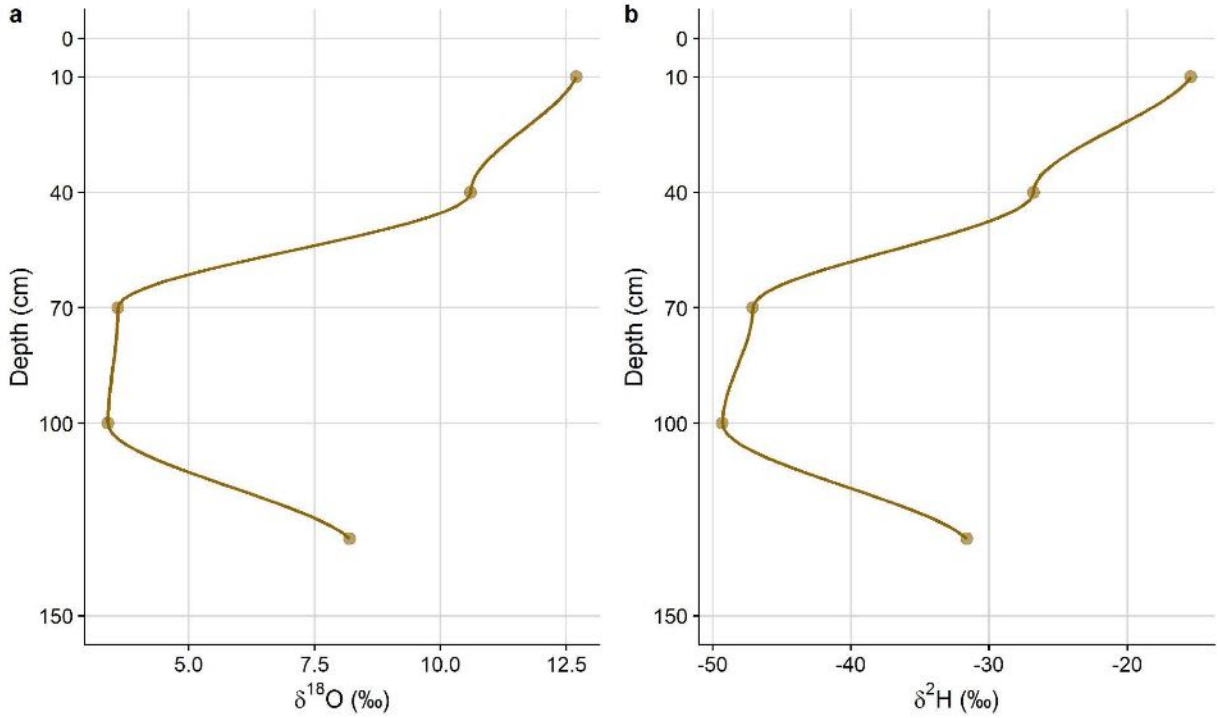


Figure D1. The $\delta^{18}O$ (a) and $\delta^{2}H$ (b) isotopic signature of soil water from different depths. From 0 to 70 cm, the isotopic signature is strongly influenced by evaporation. Between 70 - 100 cm, the signature of the soil water is more negative and thus more representative of precipitation, indicating that winter rainfall on average, percolates to this depth and has experienced less of an evaporative effect. Below 100 cm the signature is intermediate between the preceding depths, likely due to partial piston-type flow and preferential flow resulting in the mixing of older and newer waters or hydraulic redistribution of groundwater. This suggests that maximum rainwater infiltration depth is around 70 to 100 cm.

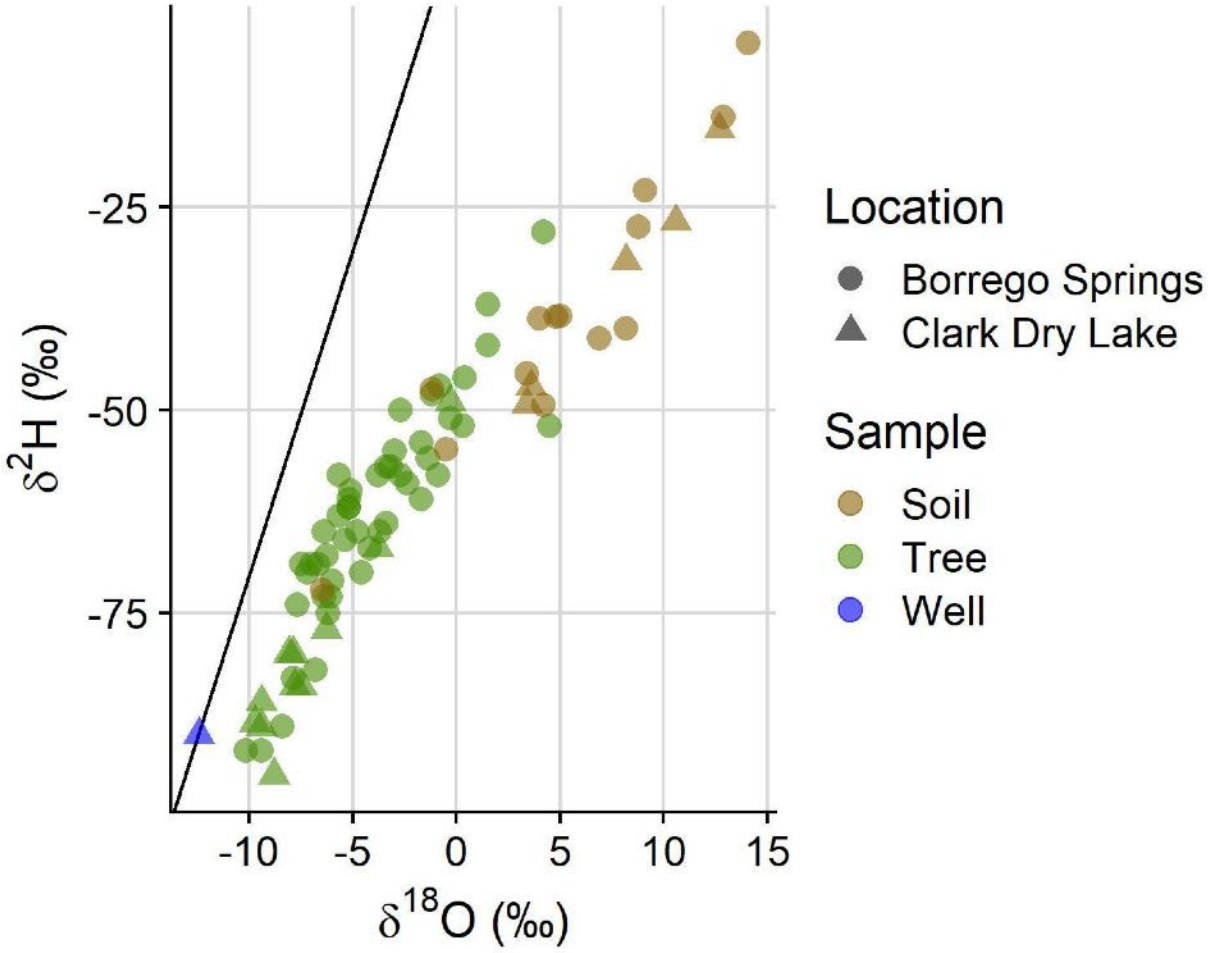


Figure D2. The relationship between $\delta^{18}O$ and $\delta^{2}H$ across all sample types. The black line indicates the Global Meteoric Water Line (GMWL), which is described by the equation: $\delta^{2}H = 8 \cdot \delta^{18}O + 10$, and represents the mean global relationship between $\delta^{2}H$ and $\delta^{18}O$ in precipitation. The alignment of the well water samples on the GMWL line indicates groundwater that originated as precipitation through recharge processes. Points to the right of this line indicate the influence of evaporation. The brown points representing soil water are farther to the right and of a lower slope than the GMWL, indicating a stronger effect of evaporation on their isotopic signature relative to the green points. The green points representing mesquite water are also to the right of the line but show little overlap with the brown points, indicating an isotopic signature that can only be explained by the mixing of soil water and well water sources.

Appendix References

Abatzoglou, J. T. (2013). Development of gridded surface meteorological data for ecological applications and modelling. *International Journal of Climatology*, *33*(1), 121-131.

Eamus, D., Fu, B., Springer, A. E., & Stevens, L. E. (2016). Groundwater dependent ecosystems: classification, identification techniques and threats. *Integrated groundwater management: concepts, approaches and challenges*, 313-346.

Fisher, J. B., Tu, K. P., & Baldocchi, D. D. (2008). Global estimates of the land–atmosphere water flux based on monthly AVHRR and ISLSCP-II data, validated at 16 FLUXNET sites. *Remote Sensing of Environment*, *112*(3), 901-919.

Gou, S., Gonzales, S., & Miller, G. R. (2015). Mapping potential groundwater-dependent ecosystems for sustainable management. *Groundwater*, *53*(1), 99-110.

Holland, R. F. (1986). *Preliminary descriptions of the terrestrial natural communities of California*. State of California, The Resources Agency, Department of Fish and Game.

Kendall M.G. (1948). *Rank correlation methods*. London, UK: Griffin.

Melton, F.S., Huntington, J., Grimm, R., Herring, J., Hall, M., Rollison, D., Erickson, T., Allen, R., Anderson, M., Fisher, J.B. and Kilic, A. (2022). OpenET: Filling a critical data gap in water management for the western United States. *JAWRA Journal of the American Water Resources Association*, *58*(6), 971-994.

PRISM Climate Group, Oregon State University, https://prism.oregonstate.edu, accessed 20 Jan 2024.

Ricotta, C., Avena, G., & De Palma, A. (1999). Mapping and monitoring net primary productivity with AVHRR NDVI time-series: statistical equivalence of cumulative vegetation indices. *ISPRS Journal of Photogrammetry and Remote Sensing*, *54*(5-6), 325-331.

San Diego Geographic Information Source (SanGIS). (2022). "ECO_VEGETATION_CN" Layer. Regional Vegetation to illustrate the vegetation communities and disturbed areas throughout San Diego County. Available at https://gis-sangis1.hub.arcgis.com/pages/download-data. Version: 13 October 2022.

Sawyer, J., Keeler-Wolf, T., & Evens, J. (2009). A manual of California vegetation, 2nd Edition. (p. 1300). Sacramento, CA. *California Native Plant Society*. Online version available at https://vegetation.cnps.org/